

# Adsorption of tetralin and hydrogenated intermediates and products on the (100) surfaces of Ir, Pt and Pd: a DFT study

Xiang Li · Madaliene S. M. Wong · Kok Hwa Lim

Received: 31 October 2009 / Accepted: 20 January 2010 / Published online: 11 February 2010  
© Springer-Verlag 2010

**Abstract** The current work presents systematic density functional theory (DFT) study on the adsorption characteristics of H, C, CH<sub>3</sub>, C<sub>2</sub>H<sub>4</sub>, C<sub>6</sub>H<sub>6</sub>, C<sub>6</sub>H<sub>10</sub>, tetralin, tetralin's plausible monohydrogenated intermediates and the hydrogenated products (1-butylbenzene, 1-methyl, 2-propylbenzene, and 1,2-diethylbenzene) involved in the selective ring opening (SRO) of tetralin on the (100) surfaces of Ir, Pt and Pd. We found that the most stable product of SRO of tetralin on the 3 metal surfaces was 1-butylbenzene. Generally, the adsorptions on 3 metal surfaces have the similar tendency, and most of the species bind most favorably to Ir compared to Pt and Pd. From our thermodynamic analysis, the overall reaction energetic for the three possible ring opening pathways are exothermic, with 1,2-diethylbenzene and 1-methyl, 2-propylbenzene being more energetically favorable compared to 1-butylbenzene.

**Keywords** DFT · Tetralin · Ir · Pt · Pd

## 1 Introduction

Facing the challenge of declining quality of crude oil, refiners have added variety of incentives to improve refining processes to meet the changing market demands and increasingly rigorous environmental regulation and fuel specifications [1–3]. This has created a growing

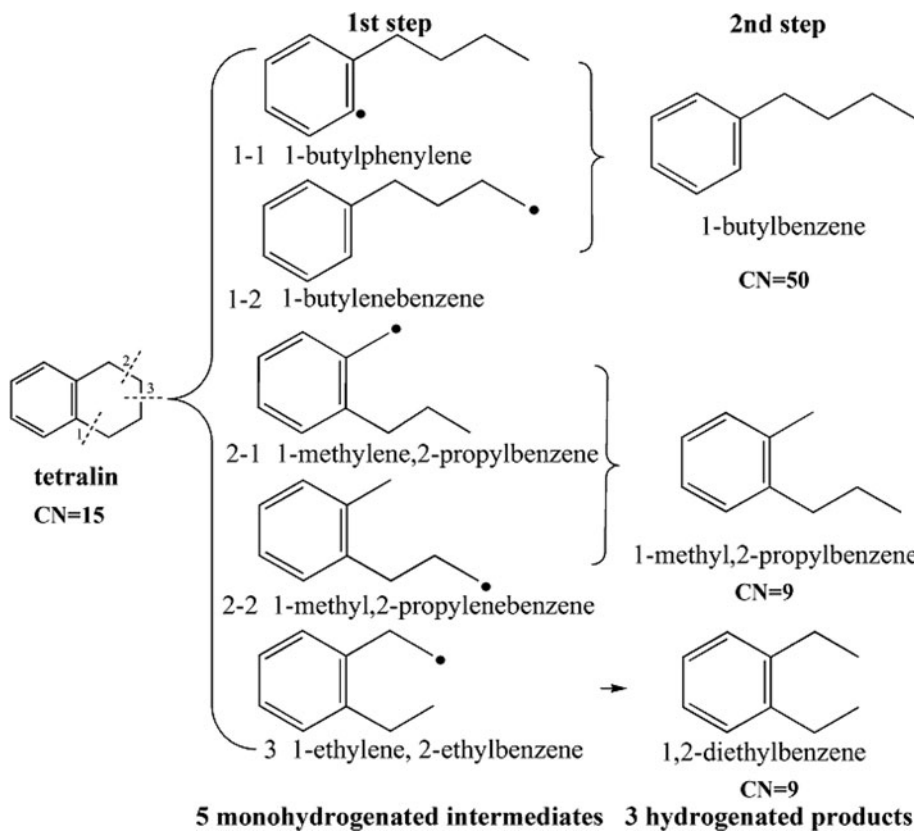
interest in the chemistry of crude oil, particularly, the upgrading of light-cycle oils by fluid catalytic cracking process that contain large amounts of aromatics such that it can be used as clean diesel fuel. Traditionally, these aromatics are treated in a two-step process on noble metal catalyst surface [4]. In this process, aromatics first undergo hydrogenation to form saturated cyclic components and then cracking to form shorter chains. However, this step tends to lead to over-cracking and hence undesired products of low cetane numbers (CN) [4]. The problem could be overcome through the selective ring opening (SRO) of cyclic hydrocarbons to form paraffins with reduced number of ring structures as well as fewer branched paraffins as illustrated in Fig. 1 [5, 6].

Since SRO process can increase the CN purposively, many researchers have done lots of studies on these reactions. In previous works [1, 5, 7–10] for the SRO reactions, researchers mainly focused on the experimental studies. Santana and coworkers [5] found that the catalysts played a crucial role in the process for CN upgrading. They illustrated that the final products of the SRO reactions may contain the branching groups, which has a significantly negative effect on CN. Unless the highly selective catalysts are employed in the reactions, the CN will be even lower than the original reactant with the branching structure [1] (see Fig. 1).

Intensive studies [8–20] have been done to find the suitable catalysts and transition metals. Ir, Pt and Pd are found to be active and selective in SRO reactions [13–20]. Jimenez-Lopez et al. [13] investigated the activity of Ni catalysts, and found that it has high hydrogenation activity and ring opening conversion under moderate temperature (648 K). Arribas and coworkers [14] observed that the Pt/ITQ21 catalyst could reduce the degree of over-cracking and increase the selectivity for ring opening products,

X. Li · M. S. M. Wong · K. H. Lim (✉)  
Division of Chemical and Biomolecular Engineering,  
School of Chemical and Biomedical Engineering,  
Nanyang Technological University,  
62 Nanyang Drive, Singapore 637459, Singapore  
e-mail: kohwa@ntu.edu.sg

**Fig. 1** Selected tetralin's ring-opening paths. CN cetane number



which have higher yield and CN than other products derived from Pt/USY and Pt/Beta. Rodriguez et al. [20] employed bimetallic catalysts (Pd–Pt), and observed that its selectivity and activity are better than the monometallic catalyst.

In contrast to the experimental results, to the best of our knowledge, theoretical study of SRO reactions is still absent. The mechanisms of the C–C bond breaking and the adsorption characteristics on the catalyst surfaces for cyclic hydrocarbons need to be investigated at the molecular level. As such, the objective of this paper is to understand the adsorption characteristics of cyclic hydrocarbons on the three transition metal (Ir, Pt and Pd) surfaces as the first step to understand the SRO reactions. This is because adsorption of cyclic hydrocarbons on transition metal surfaces is a key elementary step for possible SRO reactions. Here, we have chosen tetralin-(1, 2, 3, 4-tetrahydronaphthalene) as the model molecule for the study as it is a common component in light-cycle oil and contains three different C–C bonds. Our work is organized as follows. In Sect. 2, we present the computational methods and the models employed in the work. In Sect. 3, we discuss the adsorption characteristics and reaction energetics of tetralin, its monohydrogenated intermediates and the hydrogenated products as well as related atom and molecules related to tetralin's

structure (i.e. H, CH<sub>3</sub>, C<sub>2</sub>H<sub>4</sub>, C<sub>6</sub>H<sub>6</sub>, C<sub>6</sub>H<sub>12</sub>). Finally, we will summarize our results in Sect. 4.

## 2 Computational details and surface models

All calculations were performed using the plane-wave based Vienna ab initio simulation package (VASP) [21–23] using the PBE generalized-gradient approximation for the exchange-correlation functional [24]. The interaction between atomic cores and electrons was described by the projector augmented wave method (PAW) [25, 26]. For integrations over the Brillouin zone, we combined a (3 × 3 × 1) Monkhorst–Pack grid [27]. Throughout, we adopt an energy cut-off of 400 eV as it is found in previous studies to be sufficient for our current purposes [28–34]. Coordinates of adsorbates and substrate atoms included in the optimization procedure were optimized until the force acting on them was < 0.01 eV/Å.

Extended surfaces of Ir (100), Pt (100) and Pd (100) were modeled by four-layer slabs. Each unit cell consisted of 18 atoms per layer to enable us to consider surface coverage as low as 1/18. The vacuum spacing between the periodically repeated slabs was set to ~1 nm. All substrate atoms are fixed for all the calculations. Adsorbates were positioned on one side of the slab for adsorption studies.

The binding energy (BE) of an adsorbate to the metal substrate is calculated as follows:

$$BE = E_{ad} + E_{sub} - E_{ad/sub}$$

where  $E_{ad/sub}$  is the total energy of the adsorption complexes,  $E_{ad}$  and  $E_{sub}$  are the total energies of the adsorbate in the gas phase and of the clean substrate, respectively. With this definition, a positive value implies a release of energy or a favorable adsorption.

The reaction energies (RE), taking place on catalysts' surface, is calculated based on the following equation:

$$RE = \Sigma(BE)_R + (\Sigma(E_{ad})_P - \Sigma(E_{ad})_R) + \Sigma(BE)_P$$

where  $\Sigma(BE)_P$  and  $\Sigma(BE)_R$  are the summation of binding energies of all products and reactants involved in the reactions, respectively and  $(\Sigma(E_{ad})_P - \Sigma(E_{ad})_R)$  is the gas phase reaction energy. With this definition, a negative value implies an exothermic surface reaction.

### 3 Results and discussion

The optimized lattice constant for bulk Ir is 388 pm, in good agreement with previous reported theoretical value of 385 pm with the PW91 functional [35] and experimental value of 384 pm [36]. For Pt and Pd the optimized lattice constants are 396 and 398 pm from our previous work [37], respectively. For adsorption studies of small atoms and molecules (H, C, CH<sub>3</sub>, C<sub>2</sub>H<sub>4</sub>), three high symmetrical adsorptions sites are studied (see Fig. 2).

#### 3.1 Adsorption complexes on the three (100) metal surfaces

For the ease of comparison and discussion, the most stable bonding energies of the atoms, small molecules, tetralin, its mono-hydrogenated intermediates and hydrogenated products are tabulated in Table 1.

##### 3.1.1 Atomic H

Previous studies on Ir (100) [38] and (111) [39] surfaces suggest that the least stable site for H atom adsorption is the hollow site. Our calculated corresponding binding energy for the hollow site on Ir (100) surface is 257 kJ/mol, smaller than 275 and 288 kJ/mol obtained for top and bridge sites respectively. These values are comparable to the previously reported values of 251, 275 and 283 kJ/mol for hollow, bridge and top sites, respectively on the Ir (100) surface [38]. Krekelberg et al. [39] have studied the atomic H adsorption on Ir (111) surface using PW91 functional [40], and they found that the top site is the most favorable with binding energy of 263 kJ/mol, slightly lower than the

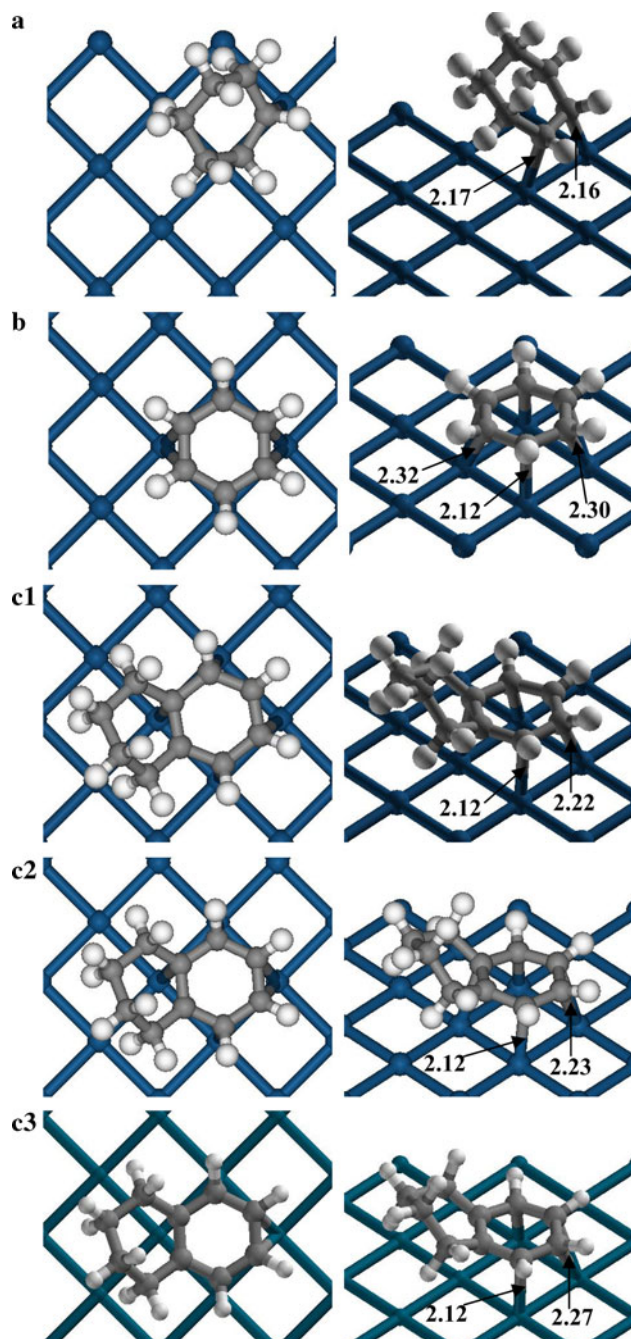


**Fig. 2** The top and side views of cyclohexene (*Ir*), benzene (*Ir*) and tetralin (all 3 surfaces). Pertinent bond distances showed are in Å. Cyan atoms: Iridium; gray atoms: Carbon; white atoms: Hydrogen. **a** cyclohexene, **b** benzene, **c** tetralin. 1, 2, 3 stands for Ir, Pt and Pd, respectively

(100) surface as the Ir atoms are more coordinated on the (111) surface compared to (100) surface and hence binds less strongly to H. Similarly, adsorptions behavior of H are found on Pt (100) with surface binding energies of 282, 262 and 246 kJ/mol for bridge, top and hollow sites, respectively in our previous study [37]. On Pd (100) surface,

**Table 1** Binding energies (kJ/mol) on the (100) surfaces of Pd, Pt and Ir

Adsorbates	Ir	Pt	Pd
H	288	282	265
C	787	721	755
CH <sub>3</sub>	205	195	167
C <sub>2</sub> H <sub>4</sub>	137	125	93
Cyclohexene	114	96	67
Benzene	244	183	216
Tetralin	230	168	131
1-Butylphenylene	419	329	270
1-Butylenebenzene	251	199	134
1-Methylene, 2-propylbenzene	398	322	273
1-Methyl, 2-propylenebenzene	259	192	149
1-Ethylene, 2-ethylbenzene	476	395	324
1-Butylbenzene	236	171	131
1-Methyl, 2-propylbenzene	229	167	127
1,2-Diethylbenzene	221	159	120

The last five adsorbates are the monohydrogenated intermediates

H atoms prefer high-coordination adsorption sites [37, 41] with binding energies of ~265 kJ/mol for both the bridge and hollow sites, close to the reported experimental value of 259 kJ/mol [42].

The unfavorable hollow adsorption site for H adsorption on Ir and Pt can be attributed to the excessive stretching of the H–Ir and H–Pt bonds at the hollow sites. From the covalent radius of H, Ir, Pt and Pd, the expected H–metal bond distances are 1.72 Å (H–Ir), 1.67 Å (H–Pt) and 1.70 Å (H–Pd) [43]. Here, our optimized H–metal bond distances at the hollow sites are 2.06 Å (H–Ir), 2.05 Å (H–Pt) and 2.00 Å (H–Pd). In comparison, the bond distances on Ir, Pt and Pd are stretched by 0.34 Å (20%), 0.38 Å (23%) and 0.30 Å (18%), respectively. Therefore, this destabilized the hollow sites on Ir and Pt (100) surfaces in comparison to the Pd (100) surface where H prefers highly coordination sites [44–46]. The biggest energy gap between most and least stable sites among the three surfaces is about ~45 kJ/mol, which implies that the H atom can easily diffuse on the transition metal surfaces.

### 3.1.2 Atomic C

C adsorption is highly favored on the hollow sites and least stable on the top sites on all three surfaces, and the energy differences between these two sites on the Ir, Pt and Pd surfaces are more than 240 kJ/mol, meaning that C atom would not be as mobile as H on these surfaces. These are in good agreements with other studies where adsorbed C atom tends to occupy the high-coordination sites on transition metals [28, 41, 47–49]. Adsorbed C on Ir (100) surface

exhibits the highest binding energy of 801 kJ/mol followed by Pd (100) (769 kJ/mol) and Pt (100) (735 kJ/mol) surfaces, such high binding energy means that the three metals are rather susceptible to carbon poisoning, especially Ir.

Our current binding energies are consistent with previous reported values of 790 kJ/mol on Ir (100) [50] hollow site using PW GGA-II [51] functional and greater than the binding energies of ~650 and ~640 kJ/mol on Pt (111) [52] and Pd (111) [28] hollow sites using the PW91 functional [40]. This is because C prefers high coordination sites and the coordination at the hollow sites for (100) and (111) surfaces are 4 and 3, respectively. Here, we see that adsorbed C atom has a higher binding energy on Pd compared to Pt surface, because on the Pd surface, the adsorbed C atom is closer to the surface leading to enhanced interaction with the second layer Pd atom. Here, we found that the bond distance between C and the second layer Pd and Pt atoms are 2.03 and 2.36 Å, respectively, giving the adsorbed C on Pd surface an effective coordination number of 5. However, such minimal does not exist for C adsorption on Pt.

### 3.1.3 Methyl CH<sub>3</sub>

Methyl prefers to be adsorbed on top site among all three metal surfaces. Our calculated binding energies for the most stable CH<sub>3</sub> adsorption complex on Ir, Pt and Pd are 205, 195 and 167 kJ/mol, respectively. This is comparable to previously reported results on the (111) surfaces of Ir, Pt and Pd where the reported binding energies on top sites are 181 kJ/mol [39], 196 kJ/mol [52] and 170 kJ/mol [28], respectively. In our study, we also observed that starting the geometry optimization of CH<sub>3</sub> at other high symmetry adsorption site would end up with methyl at the top site for all the three (100) surfaces.

On all the three surfaces, methyl is bonded to the substrates through the carbon atom and hence it features the same binding trend as C, that is the binding energies follow the trend Ir (100) > Pt (100) > Pd (100).

### 3.1.4 Ethylene C<sub>2</sub>H<sub>4</sub>

Ethylene usually has two common configurations adsorbing on the metal surfaces via di- $\sigma$  bonding where two C atoms are bonded to two adjacent metal atoms and  $\pi$  bonding (two C atoms are both bond to one metal atom) [53–55]. In our study, C<sub>2</sub>H<sub>4</sub> favors the di- $\sigma$  bonding configuration with binding energy of 137, 125 and 93 kJ/mol, on Ir, Pt and Pd (100) surfaces, respectively. To the best of our knowledge, there are limited reports on Ir surfaces [56, 57] and there are no previous theoretical studies of ethylene adsorption on Ir surfaces. Previous reports of ethylene adsorption on Pt and Pd (111) surfaces [53–55] reported that the di- $\sigma$  bonding configuration is more favorable

comparing to the  $\pi$  bonding configurations. The binding energies of ethylene on Pt (111) surface reported by Hirsch et al. [58] for di- $\sigma$  and  $\pi$  configurations are 101 and 65 kJ/mol, respectively, which are comparable with 125 and 91 kJ/mol in our study. Mittendorfer et al. [59] have studied the adsorptions on both Pt and Pd (111) surfaces with similar binding energies (106 and 84 kJ/mol, respectively) with the di- $\sigma$  bonding mode. Both the above studies on (111) surfaces illustrated that the di- $\sigma$  bonding is energetically favorable than  $\pi$  bonding.

### 3.1.5 Cyclohexene $C_6H_{10}$

Cyclohexene can be perceived as a derivative of ethylene hence we would expect their adsorption characteristics to be similar. To the best of our knowledge, no theoretical studies have been reported for cyclohexene adsorption on Ir surfaces. In our current study, we found that cyclohexene favors the di- $\sigma$  configuration on all the three surfaces with adsorption energies of 114, 96 and 67 kJ/mol on Ir, Pt and Pd (100) surfaces, respectively. This is in agreement with previous reports on Pt (111) [60] that cyclohexene prefers the di- $\sigma$  configurations with adsorption energy of 81 kJ/mol. Similar adsorption complexes on Pt and Pd (111) surfaces have also been reported with adsorption energy of 108 and 81 kJ/mol, respectively [61]. Here, comparing the adsorption energies of ethylene and cyclohexene, we found that the ethylene is generally more stable by 25 kJ/mol. This can be understood from the more bulky cyclohexene structure where it poses more steric effect compared to ethylene.

### 3.1.6 Benzene $C_6H_6$

As benzene can be seen as containing three C=C double bonds, its adsorption feature should have the similar manner as ethylene's. Therefore, benzene maximized its di- $\sigma$  bonding during interaction with metal surfaces and for the most stable adsorption complexes on Ir, Pt and Pd (100) surfaces, there are 2 di- $\sigma$  bonds with binding energies of 243, 183 and 216 kJ/mol, respectively and the molecular plane parallel to the surfaces.

Adsorption of benzene on noble metal surfaces has been extensively studied by a number of experimental [62–64] and theoretical [61, 65–69] studies as it is a classical representation for aromatics. Nevertheless, previous theoretical researches [61, 65–69] deal primarily with the (111) surfaces of Pt and Pd. On all the surfaces, benzene binds to the surface with two di- $\sigma$  bonds. The similar geometries show that benzene has a common adsorption feature on all investigated surface. Compared with ethylene, benzene has one more di- $\sigma$  bond. Although the  $\pi$  bonds affect the di- $\sigma$  configuration to be slightly distorted, the binding energy of benzene is larger than ethylene and cyclohexene.

Previous spectroscopy techniques such as high-resolution electron energy loss spectroscopy (HREELS), reflection-adsorption infrared spectroscopy (RAIRS) and low-energy electron diffraction (LEED) [63, 64] concluded that benzene adsorbed on Pt (111) with its ring parallel to the surface, in agreement to our most favorable adsorption configurations.

Previous quantum chemistry calculations on Pt (111) surface have found the most stable site is at the bri30°site (bri stand for the bridge site, and 30° presents the angles of C–C bonds being rotated with respect to the atomic directions on the surface), the data from Morin's studies is 87 kJ/mol [62]. Our binding energy on Pt (100) surface is ~183 kJ/mol, which is much higher than the values predicted by Morin. Similar energy gap also exists on Pd surfaces in Ref. [61] (216 vs. 115 kJ/mol). Our additional calculation for benzene adsorption on Pt (111) shows the highest binding energy is ~90 kJ/mol, which is very close to Morin's result. Unlike simple atoms and molecules, the adsorption sites for benzene between (100) and (111) are quite different. As discussed in Ref. [55], benzene has the most stable structure at bridge site on Pt and Pd (111) surfaces. The configuration contains two  $\pi$  bonds. According to the discussion in ethylene adsorption, di- $\sigma$  bonds are more stable than  $\pi$  bonds. Hence the binding energies on (111) surfaces are significantly lower than (100) surfaces.

It is notable that benzene is the only molecule where its binding energy is higher for Pd than Pt in our study (shown in Table 1). This is in agreement with the earlier results for Pt (111) and Pd (111) surfaces [61] with adsorption energies of 87 and 115 kJ/mol, respectively. Due to the mismatch of lattice constant with different metals, the molecule need to find an optimal binding with the surface and hence undergoes distortion from its gas phase structure. This will require energy and hence lower the stability of the adsorption complexes. Here we infer the data of binding energies for benzene could be due to the greater distortion of benzene on Pt (100) than Pd (100) surface (distortion energy 140 kJ/mol for Pt and 88 kJ/mol for Pd, energy difference of 52 kJ/mol). This deviation from the configuration in gas phase is so dominant that the interaction of the molecule and the substrate is insufficient to compensate for the loss of energy due to distortion. The outcome is the larger adsorption energy on Pd than Pt surface.

### 3.1.7 Tetralin, $C_{10}H_{12}$

To the best of our knowledge, only limited experimental studies have been reported on tetralin adsorption on metals surfaces [15, 70] and there are no theoretical studies reported.

The largest binding energy of 230 kJ/mol is exhibited on Ir (100) surface. The binding energies are 168 and 131 kJ/mol on the (100) surfaces of Pt and Pd, respectively. Since tetralin contains a cyclohexene and a benzene ring, it possesses the adsorption characteristics of both benzene and cyclohexene. Hence we will compare our results with benzene adsorption and cyclohexene here. The optimized structures of cyclohexene, benzene and tetralin on Ir surface are shown in Fig. 2.

From Fig. 2 we observed that instead of a di- $\sigma$  configuration for the tetralin's "cyclohexene C=C bond", only one C–Ir bond is formed to the surface. This is mainly due to the steric effect of the "cyclohexene" part of tetralin. Remember that benzene can form two di- $\sigma$  configurations, hence in this case due to steric effects, it prefers to use the C=C bonds not associated to the "cyclohexene" to be bounded to the surface. In addition, steric effect from the "cyclohexene" ring obstruct the formation of additional  $\pi$  bonds to the surface leading to lower binding energies compared to the benzene analog on the three surfaces.

From Fig. 2 we observed that the adsorption configuration of the benzene analog of tetralin are very similar to those of benzene adsorption. On Ir and Pt (100) surfaces, the benzene rings bind to the surface with two di- $\sigma$  bonds. On Pd (100) surface, due to the weaker C–metal interaction and steric effect from tetralin's side chain only one di- $\sigma$  bond is formed. As a result, the binding energy of tetralin on Pd is lower than Pt surface, in contrast to benzene on the surfaces.

Based on the above discussion, we can get the following useful information. The two rings of tetralin hold similar adsorption features of the cyclohexene and benzene. Hence the final configuration of tetralin attributes to the combination of these two molecules, and this corroborates our early speculation in the first paragraph. Meanwhile, the steric effect from the side chain lower the binding energies of tetralin. These deviations results in the lower binding energy than benzene.

### 3.1.8 Mono-hydrogenated intermediates

For the mono-hydrogenated intermediates, binding energies generally follow the trend of being the most strongly adsorbed on Ir, followed by Pt and Pd surface (Table 1). In general, the adsorption geometries are similar on all three surfaces. For the ease of understanding, the most stable adsorption complexes on Ir (100) are illustrated in Fig. 3 with pertinent geometries listed for all the three surfaces.

**3.1.8.1 1-Butylphenylene** 1-Butylphenylene—the intermediates for pathway 1–1, has the most stable complex (shown in Fig. 3) on Ir, Pt and Pd with binding energies of

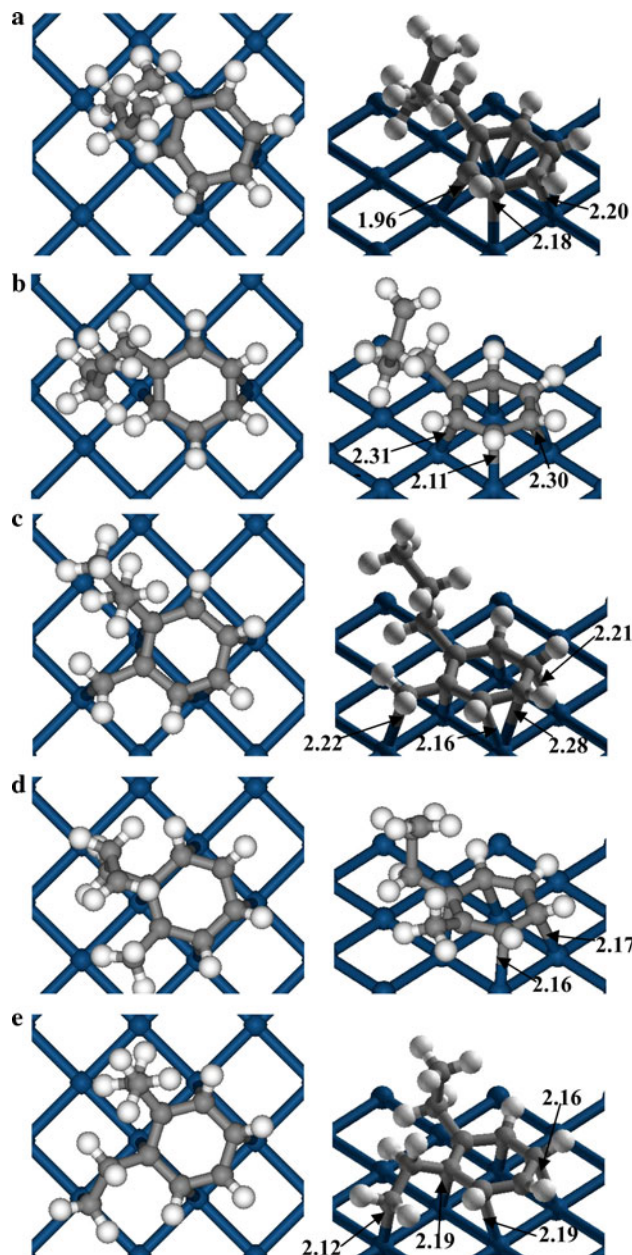


**Fig. 3** Top and side view of most stable intermediates on Ir (100) surfaces. Pertinent bond distances showed are in Å. Cyan atoms: Iridium; gray atoms: Carbon; white atoms: hydrogen. Only first layer of Ir is shown for clarity. **a** 1-Butylphenylene, **b** 1-butylenebenzene, **c** 1-methylene, 2-propylbenzene, **d** 1-methyl, 2-propylbenzene, **e** 1-ethyl, 2-ethylenebenzene

419, 329 and 270 kJ/mol, respectively. From the geometry of 1-butylphenylene, the radical carbon on the aromatic ring binds to the metal surface (shown in Fig. 4). This binding distorts the benzene ring to a great extend (see Fig. 4), most significantly, the shortening of C–metal bond (1.96 and 2.18 Å from 2.22 and 2.13 Å for tetralin) leading to stronger binding energies (more than 150 kJ/mol) compared to tetralin.

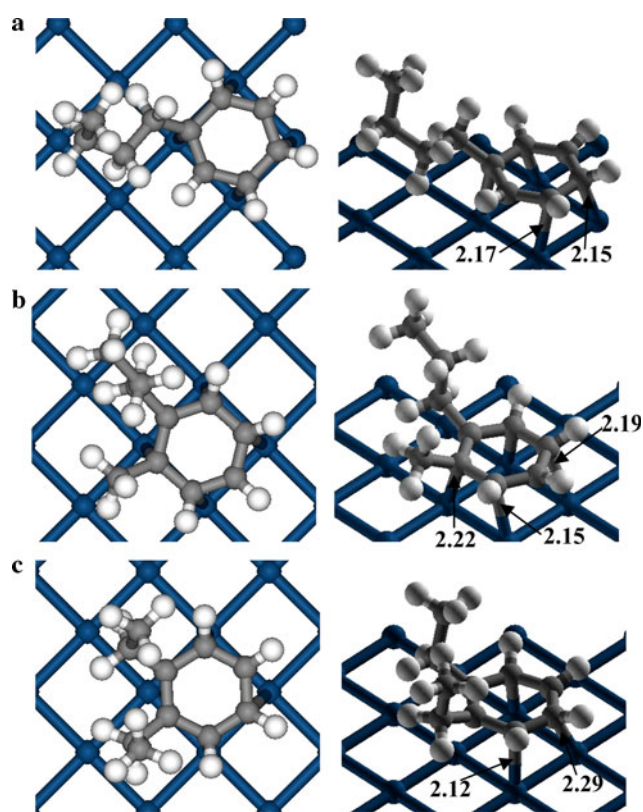


**Fig. 4** *Top and side* view of the most stable products on Ir (100) surfaces. Pertinent bond distances showed are in A. Cyan atoms: Iridium; gray atoms: Carbon; white atoms: hydrogen. Only first layer of Ir is shown for clarity. **a** 1-Butylbenzene, **b** 1-methyl,2-propylbenzene, **c** 1, 2-diethylbenzene

**3.1.8.2 1-Butylenebenzene** Optimized adsorption complexes of 1-butylenebenzene (pathway 1–2) on Ir, Pt and Pd are bounded to the surfaces with binding energies of 251, 199 and 134 kJ/mol, respectively. The radical C at the end of the butylene group does not bind to the surface due to steric effect as a long side chain (4 carbons are included) of the benzene ring, leaving the binding energies lower than 1-butylphenylene and slightly higher than tetralin, as it contains less strain.

**3.1.8.3 1-Methylene, 2-propylbenzene** Most stable adsorption complexes of 1-methylene, 2-propylbenzene (pathway 2–1) have binding energies of 398, 322 and 273 kJ/mol on Ir, Pt and Pd (100) surfaces, respectively. Compared with tetralin, the benzene ring has no significant distortion on the surface. We note that the short branched chain binds to the metal (shown in Fig. 3) by the terminal radical C. As a result, the benzene ring has been shifted slightly (compared to tetralin) and stabilized by this additional C-metal bond leading to higher binding energies of about 100 kJ/mol compared to tetralin.

**3.1.8.4 1-Methyl, 2-propylenebenzene** 1-Methyl, 2-propylenebenzene (pathway 2–2) binds to the Ir, Pt and Pd (100)

surfaces with binding energies of 259, 192 and 149 kJ/mol, respectively. The benzene ring is quite similar to tetralin's (Fig. 3). Similar to 1-butylenebenzene, the radical C is on the long branched chain (propylene), which has been kept away from the surface (see Fig. 3) due to steric effect and hence the binding energies are comparable to those of tetralin.

**3.1.8.5 1-Ethylene, 2-ethylbenzene** Compared with the previous four intermediates, 1-ethylene, 2-ethylbenzene (pathway 3) has the largest binding energies on the (100) surfaces of the three metals studied: 473 kJ/mol for Ir, 393 kJ/mol for Pt and 324 kJ/mol for Pd. The radical C on one side chain binds to the surface to form a new C-metal bond. The other saturated side chain tends to keep away from metal surface. The additional C-metal bond from the side chain results in the stronger (>190 kJ/mol) binding energies than tetralin.

### 3.1.9 Hydrogenated products

The hydrogenated products are similar to tetralin except of the side chains, hence we would expect their adsorption properties to be similar.

**3.1.9.1 1-Butylbenzene** 1-Butylbenzene is the most preferred hydrogenated product among the three possible products for the ring opening of tetralin side chain. The binding energies of the most stable adsorption complexes on Ir, Pt and Pd surfaces are 236, 171 and 131 kJ/mol, respectively comparable to tetralin adsorption. The configuration of the benzene ring for 1-butylbenzene is very close to that in tetralin since the main interactions with the surface is via the benzene ring.

**3.1.9.2 1-Methyl, 2-propylbenzene** 1-Methyl, 2-propylbenzene is the second most favored adsorption complex among all the surfaces. It has binding energies of 229, 167 and 127 kJ/mol on Ir, Pt and Pd (100) surfaces, respectively. Here, the binding energies are all slightly lower than those of tetralin. By comparing the geometry of these two complexes, we can see they have quite close configurations of the benzene rings (shown in Figs. 2, 4 for tetralin and 1-methyl, 2-propylbenzene, respectively).

**3.1.9.3 1,2-Diethylbenzene** The 1,2-diethylbenzene is the least stable product on Ir, Pt and Pd (100) surfaces with the binding energies of 221, 159 and 120 kJ/mol, respectively. Compared with tetralin, all adsorption energies are slightly lower. We found that the case is similar to that of 1-methyl, 2-propylbenzene, i.e. the geometry (shown in Figs. 2, 4) and the deviation from the aromaticity for this product and tetralin are very similar.

### 3.2 Thermodynamic analysis

Table 2 summarized the reaction energies for the two steps tetralin hydrogenation process. In general, all the overall hydrogenation processes on the three surfaces are exothermic for all the products. Since the kinetics calculations are not involved in our current study, we are trying to estimate the rate determining elementary reaction through thermodynamics consideration as currently. From the tabulated data, the rate determining step (RDS) is likely to be the first mono-hydrogenation for all the three products as they are significantly more endothermic compared to the second hydrogenation step.

For the formation of 1-butylbenzene, pathway 1–1, the reaction energies are very endothermic: 108, 115 and 97 kJ/mol on Ir, Pt and Pd surfaces, respectively. In addition, pathway 1–2 on Ir, Pt and Pd surfaces are also very endothermic with reaction energies 229, 218 and 231 kJ/mol, respectively. This means that the likely RDS for the formation of 1-butylbenzene is pathway 1–1. However, with these highly endothermic processes, we would expect the selectivity for 1-butylbenzene in the SRO process to be the lowest. These are in agreement with experimental finding of decalin [71] and indan [1] on Pt–Ir based catalysts where the selectivity of butylcyclohexane and *n*-propylbenzene, respectively are the lowest among the ring opening products.

For formation of 1-methyl, 2-propylbenzene, pathway 2–1 is energetically more favorable compared to pathway 2–2. In fact, the reaction energies on pathway 2–1 are slightly exothermic and they are –11, –8 and –4 kJ/mol on Ir, Pt and Pd respectively. In contrast, pathway 2–2 is very endothermic with reaction energies of 216, 206 and 208 kJ/mol on Ir, Pt and Pd surfaces respectively. The favorable energetic for pathway 2–1 means that it is likely the RDS for 1-methyl, 2-propylbenzene coupled with 1-methyl, 2-propylbenzene being the energetically most favorable product, we would expect it to have the highest selectivity for the SRO reaction, in line with experimental reports of 70% selectivity of 2-ethyltoluene for indan ring opening reaction on Pt–Ir based catalysts [1, 71].

**Table 2** Calculated reaction energies (in kJ/mol) of various reaction paths (see Fig. 1) on Pd, Pt and Ir (100) surfaces

	1st step			2nd step		
	Ir	Pt	Pd	Ir	Pt	Pd
(1–1)	108	115	97	–186	–193	–179
(1–2)	229	218	231	–307	–296	–313
(2–1)	–11	–8	–4	–63	–66	–68
(2–2)	216	206	208	–290	–280	–280
(3)	–6	–2	–9	–64	–68	–68

1,2-Diethylbenzene is a symmetric compound and hence it has only pathway 3–1 in the ring opening reactions with reaction energies of –6, –2 and –9 kJ/mol on Ir, Pt and Pd respectively. According to these data, 1,2-diethylbenzene is energetically favorable on all investigated surfaces. This corroborates with the experimental trend for decalin [71] and indan [1] ring opening reactions on Pt–Ir based catalysts.

### 4 Conclusions

In the current work we have systematically studied the adsorption of tetralin and its relevant hydrogenated intermediates and products adsorbates on the (100) surfaces of Ir, Pt and Pd.

In summary, our data for all adsorbates indicate that the adsorption energies on (100) surfaces generally follow the trend: Ir > Pt > Pd with the exception of C and benzene where binding energies are larger on Pd (100) surface compared to Pt (100) surface. C=C double bonds have a propensity to form the di- $\sigma$  bond on all surfaces. Among the hydrogenated intermediates, 1-butylenebenzene and 1-methyl, 2-propylenebenzene are the destabilized by at least  $\sim$  130 kJ/mol due to steric effects that prevent their radical side chain carbon from binding to the surface leading to a difference of binding energy. The hydrogenated products adsorbed slightly weaker on the surfaces compared to tetralin as their adsorption configuration are similar, but with steric interactions from the side chain.

We have studied the energetic of three different ring opening pathways of tetralin on Ir, Pt and Pd (100) surfaces. We found that the first hydrogenation step is likely to be the RDS for the ring opening process. Here, we found that the thermodynamics of the first hydrogenation step is among the leading factor for the selectivity of the tetralin ring opening process.

**Acknowledgments** X.L. acknowledges funding from China Scholarship Community (No. [2008]3019) and NTU. This project is funded by NTU grant M58120000 and RG 110/06.

### References

- Du H-B, Fairbridge C, Yang H et al (2005) Appl Catal A Gen 294:1–21
- Decroocq D (1997) J French Inst Petrol 52:5
- Cooper BH, Donnis BBL (1996) Appl Catal A 137:203
- McVicker G, Daage M, Touvelle M et al (2002) J Catal 210:137–148
- Santana RC, Do PT, Santikunaporna M et al (2006) Fuel 85:643–656
- Arribas MA, Corma A, Díaz-Cabañas MJ et al (2004) Appl Catal A Gen 273:277–286
- Liu X, Smith KJ (2008) Appl Catal A Gen 335:230–240

8. Fujii H, Osa Y, Ishihara M et al (2008) *Bioorg Med Chem Lett* 18:4978–4981
9. Sheldrake GN, Soissons N (2006) *J Org Chem* 71:789–791
10. Santikunaporn M, Alvarez WE, Resasco DE (2007) *Appl Catal A Gen* 325:175–187
11. Galperin LB, Bricker JC, Holmgren JR (2003) *Appl Catal A Gen* 239:297–304
12. Arribas MA, Concepción P, Martínez A (2004) *Appl Catal A Gen* 267:111–119
13. Eliche-Quesada D, Mrida-Robles J, Jimnez-Lopez A et al (2003) *Langmuir* 19:4985–4991
14. Arribas MA, Corma A, Martínez A et al (2004) *Appl Catal A Gen* 273:277–286
15. Ma H, Yang X, Tian Z et al (2007) *Catal Lett* 116:149–154
16. Baird WC Jr, Chen JG, GB McVicker (2003) US Patent 6,623,625
17. Baird WC Jr, Chen JG, McVicker GB (2003) US Patent 6,623,626
18. Baird WC Jr, Klein DP, Touvelle MS et al (2003) US Patent 6,586,650
19. Baird WC Jr, Klein DP, Touvelle MS et al (2003) US Patent 6,589,416
20. Carrión MC, Manzano BR, Rodríguez-Castellón E et al (2005) *Green Chem* 7:793–799
21. Kresse G, Furthmüller J (1996) *Phys Rev B* 54:11169
22. Kresse G, Hafner J (1993) *Phys Rev B* 47:558
23. Kresse G, Furthmüller J (1999) *Comput Mat Sci* 6:15
24. Perdew JP, Burke K, Ernzerhof M (1996) *Phys Rev Lett* 77:3865
25. Blöchl PE (1994) *Phys Rev B* 50:17, 953
26. Kresse G, Joubert D (1999) *Phys Rev B* 59:1758
27. Monkhorst HJ, Pack JD (1976) *Phys Rev B* 13:5188
28. Chen ZX, Lim KH, Rösch N et al (2004) *Langmuir* 20:8068–8077
29. Chen Z-X, Lim KH, Neyman KM, Rösch N (2004) *Phys Chem Chem Phys* 6:4499–4504
30. Chen Z-X, Lim KH, Neyman KM, Rösch N (2005) *J Phys Chem B* 109:4568–4574
31. Lim KH, Chen Z-X, Neyman KM, Rösch N (2006) *J Phys Chem B* 110:14890–14897
32. Lim KH, Moskaleva LV, Rösch N (2006) *ChemPhysChem* 7:1802–1812
33. Lim KH, Chen Z-X, Neyman KM, Rösch N (2006) *Chem Phys Lett* 420:60–64
34. Lim KH, Neyman KM, Rösch N (2006) *Chem Phys Lett* 432:184–189
35. Chen ZX, Neyman KM, Gordienko AB et al (2003) *Phys Rev B* 68:75417
36. Ashcroft NW, Mermin ND (1976) Solid state physics. Saunders College Publishing, Orlando
37. Yue CMY, Lim KH (2009) *Catal Lett* 128:221–226
38. Lerch D, Klein A, Heinz K et al (2006) *Phys Rev B* 73:1–11
39. Krekelberg WP, Greeley J, Mavrikakis M (2004) *J Phys Chem B* 108:987–994
40. Wang Y, Perdew JP (1991) *Phys Rev B* 44(24):13298–13307
41. Yudanov IV, Neyman KM, Rösch N (2004) *Phys Chem Chem Phys* 6:116
42. Shustorovich E (1990) *Adv Catal* 37:101
43. Allen FH, Kennard O, Watson DG et al (1987) *J Chem Soc Perkin Trans 2*:S1–S9
44. Marvikakis M, Hammer B, Nórshov JK (1998) *Phys Rev Lett* 81:2819
45. Bo JY, Zhang S, Lim KH (2009) *Catal Lett* 129:444–448
46. Foo ASY, Lim KH (2009) *Catal Lett* 127:113–118
47. Paul JF, Sautet P (1998) *J Phys Chem B* 102:1578
48. Neyman KM, Lim KH, Chen ZX et al (2007) *Phys Chem Chem Phys* 9:3470–3482
49. Nieskens DLS, Curulla-Ferré D, Niemantsverdriet JW (2006) *Chem Phys Chem* 7:1022–1025
50. Johnson K, Ge Q, Sauerhammer B et al (2001) *Surf Sci* 478:49–56
51. Perdew JP, Chevary JA, Vosko SH et al (1992) *Phys Rev B* 46:6671–6687
52. Ford DC, Xu Y, Mavrikakis M (2005) *Surf Sci* 587:159–174
53. Bernardo CGPM, Gomes JANF (2001) *J Mol Struct (Theochem)* 542:263–271
54. Bernardo CGPM, Gomes JANF (2002) *J Mol Struct* 582:159–169
55. Pichierri F, Iitaka T, Ebisuzaki T (2001) *J Phys Chem B* 105:8149–8154
56. Kostov KL, Marinova TS (1986) *React Kinet Catal Lett* 32:141–146
57. Chakarov DV, Marinova TS (1990) *Surf Sci* 227:297–309
58. Hirschl R, Eichler A, Hafner J (2004) *J Catal* 226:273–282
59. Mittendorfer F, Thomazeau C, Rayband P et al (2003) *J Phys Chem B* 107:12287–12295
60. Saeyns M, Reyniers MF, Marin GB et al (2006) *Surf Sci* 600:3121–3134
61. Morin C, Simon D, Sautet P (2006) *Surf Sci* 600:1339–1350
62. Sautet P, Bocquet M-L et al (1994) *Surf Sci* 304:445
63. Tysoe WT, Nyberg GL et al (1983) *Surf Sci* 135, 128
64. Waddill GD, Kesmond LL (1985) *Phys Rev B* 31:8
65. Weststrate CJ, Bakker JW, Gluhoi AC et al (2007) *Surf Sci* 601:748–756
66. Lomas JR, Pacchioni G (1996) *Surf Sci* 365:297
67. Lee Wilson et al (2000) *J Phys Chem B* 104:11719
68. Morin C, Simon D, Sautet P (2003) *J Phys Chem B* 107:2995–3002
69. Koide R, Hensen EJM, Nakamura H et al (2007) *Top Catal* 45:175–179
70. Dokjampa S, Rirksonboon T, Resasco DE (2007) *Catal Today* 123:218–223
71. Mouli KC, Sundaramurthy V, Dalai AK et al (2007) *Appl Catal A Gen* 321:17–26